ON THE ORIGIN OF METALLICITY IN LYMAN-ALPHA FOREST SYSTEMS

Masashi Chiba[1]
National Astronomical Observatory, Mitaka, Tokyo 181, Japan

and

Biman B. Nath[2]
Inter-University Center for Astronomy & Astrophysics, Post Bag 4, Pune 411007, India

ABSTRACT

We investigate the hypothesis that Lyα absorption lines arise in two populations of halos — minihalos of small circular velocity ($V_c \lesssim 55$ km s^{-1}) in which star formation and metal production are inhibited by photoionization of the UV background radiation, and large galactic halos ($55 \lesssim V_c \lesssim 250$ km s^{-1}) which possess stars and metals. Based on the model of Lyα-absorbing gas confined in both populations of halos, we attempt to explain the recent observations of (1) associations of visible galaxies with Lyα lines at low redshifts $z \lesssim 1$, and (2) metal lines associated with a non-negligible fraction of low H I column density Lyα lines at $z \sim 3$. For galactic halos, we find that photoionized gas clouds confined in the pressure of ambient hot gas can produce Lyα absorptions with H I column density as low as 10^{14} cm^{-2}, and that the impact parameter of a sightline for such absorptions matches well with the observed radius of gaseous envelope in a typical luminous galaxy. Using the Press-Schechter prescription for the mass function of halos, we also show that the fraction of Lyα lines with associated metal lines can be understood in terms of the fraction of Lyα absorbers that are associated with galactic halos. In particular, the reported fraction of ~ 0.5–0.75 at $z \sim 3$ is reproduced when the boundary value of V_c to separate mini or galactic halos is $40 \sim 60$ km s^{-1}, which is consistent with the theoretical prediction of galaxy formation under photoionization. The average metallicity of both Lyα forest and damped Lyα systems at $z \sim 3$ is explained in terms of the model of halo-formation history combined with the age-metallicity relationship of Galactic halo stars. Possible methods to test this hypothesis and the other alternative scenarios are also discussed.

Subject headings: galaxies : abundances – galaxies : evolution – galaxies : intergalactic medium

---

[1]chibams@cc.nao.ac.jp

[2]biman@iucaa.ernet.in

1. INTRODUCTION

Several recent observations indicate that even the low H I column density Lyα absorption lines may not be primordial as were previously thought. High resolution observations by Cowie et al. (1995), Tytler et al. (1995) and Womble et al. (1996) show that there are metal lines (C IV) associated with Lyα absorption lines with as small H I column density as $N_{\rm HI} \sim 10^{14}$ cm^{-2} at $z \sim 3$. The fraction of the Lyα lines with $N_{\rm HI} \gtrsim 10^{14}$ cm^{-2} that are associated with metal lines is approximately $\gtrsim 0.5$ at $z \sim 3$. The median abundance of lines with $N_{\rm HI} \gtrsim 10^{14.5}$ cm^{-2} at $z \sim 3$, is found to be [C/H] ~ -2.5. Recently Songaila and Cowie (1996) have shown that the fraction of Lyα lines that are associated with metal lines, hereafter denoted as f_m, could be higher, and they have also detected the other C II, S IV, N V absorption lines in hydrogen clouds with $N_{HI} > 10^{15}$ cm^{-2}. In view of the dependence of observational sensitivity for detecting metal lines, the fraction f_m represents only a lower limit for the fraction of Lyα lines associated with 'metals'.

Another set of observations shows that at low redshifts a large fraction of Lyα absorption lines are associated with galaxies (Maloney 1992; Morris et al. 1993). Lanzetta et al. (1995b, LBTW) claimed that $\sim 60 \pm 19\%$ of the Lyα lines at $z \lesssim 1$ arise in galactic halos. The observation of Barcons et al. (1995) in which they imaged a galaxy corresponding to an absorption line, is an evidence of such associations. It is, therefore, reasonable to assume that at least a fraction of the Lyα absorption lines arise in galactic halos, and this fraction is hereafter denoted as f_g.

In the hierarchical model of structure formation, there is a continuum of halos of various masses and velocity dispersions. In this paper, we consider the hypothesis that the Lyα lines are produced in two populations of halos in this continuum – in 'minihalos' of small velocity dispersions which have not cooled and formed stars, and in large galactic halos with stars and metals. Based on this two-population model for QSO absorbers, we attempt to explain f_m in terms of f_g by the relation $f_m \sim f_g$.

There are circumstantial evidences for such a two population scenario. In the column density distribution of Lyα lines, there is a break around $N_{\rm HI} \sim 10^{15}$ cm^{-2} (see, e.g., Cristiani et al. 1995). Petitjean et al. (1993) have interpreted this break as being due to existence of two populations of Lyα lines – the lines with higher H I column density being associated with strong metal lines and with galactic halos. Recently, Fernández-Soto et al. (1996) analyzed the two-point correlation of very weak C IV absorption lines associated with high-redshift ($z \sim 2.6$) Lyα absorption systems. They found that high-redshift Lyα absorption systems traced by C IV lines are clustered in redshift, as strongly as that expected for galaxies. This suggests that many Lyα absorbers even at high redshifts may arise in galaxies.

Our primary goal in this paper is therefore to determine whether these recent observations can be understood within the framework of a two-population model for Lyα absorption systems, including their redshift evolution in the context of hierarchical structure formation. In §2, we present a model of Lyα-absorbing gas confined in both mini and galactic halos and set the prescription for determining the number of absorption lines provided by various masses of halos.

On the basis of the Press-Schechter mass function with various power spectra and cosmological parameters, we then discuss the fraction of absorption lines in minihalos and in galactic halos by comparing with the recent Keck observations in §3. The simplified approach for modeling chemical evolution of halos is also presented to predict the evolution of the average metallicity associated with Lyα lines in redshift. The discussion and conclusions are finally drawn in §4.

2. MINIHALOS AND GALACTIC HALOS

2.1. *Assumptions and definitions*

We define minihalos as halos in which baryonic gas is entirely photoionized by the external UV background and the gas is stably confined in the gravitational field of the dark matter (Rees 1986; Ikeuchi 1986). In these minihalos, the gas does not go through extensive star formation because of suppression of radiative cooling by photoionization (Efstathiou 1992). Below, we will characterise the halos by their circular velocities V_c, where the mass density of halos is dominated by extended dark matter with r^{-2} distribution. Minihalos are therefore bounded by two scales of circular velocity, $V_1 < V_c < V_2$. The lower limit is set by the sound velocity of the photoionized intergalactic medium (IGM), which is $\sim 15\,(T_{IGM}/10^4\,\mathrm{K})^{0.5}$ km s^{-1}. Halos with V_c less than this value will not have baryonic gas infall from the IGM. This is basically the Jeans mass, below which the perturbation in baryonic gas is suppressed. We take a characteristic value of $V_1 = 15$ km s^{-1} for the photoionized IGM with $T_{IGM} \sim 10^4$ K.

The upper limit V_2 is admittedly less certain. Recent numerical simulations show that photoionization severely inhibits the formation of galaxies with $V_c \lesssim 30$ km s^{-1}, and substantially decreases the mass of cooled baryons in halos with $V_c \lesssim 50$ km s^{-1} (Thoul and Weinberg 1996). They also find that above $V_c \sim 75$ km s^{-1} photoionization of the IGM does not have any significant effect. For the reasons described in the next subsection, we will use a canonical value of $V_2 = 55$ km s^{-1} and examine the effect of changing V_2 over its possible range. In fact, we later ask the question whether or not one can *determine* the value of V_2 from the observations. In brief, then, we assume that halos with $V_c < V_2 \sim 55$ km s^{-1} do not undergo vigorous star formation, and call them minihalos in this paper.

We will call the halos with circular velocity larger than V_2, the galactic halos. Our results are not sensitive to the upper limit of the circular velocity for galactic halos, and we will use a value of $V_3 = 250$ km s^{-1} as an upper limit. Below, we will associate these halos with Lyα lines which have corresponding metal lines. It is true that the division of halos into the above categories of mini and galactic halos is rather ad hoc. However, it is most likely to be close to the real picture for the above mentioned reasons.

For the gas associated in galactic halos, the virial temperature T for $V_c \gtrsim V_2 \sim 55$ km s^{-1} is above 10^5 K [$T \sim 10^5 (V_c/55 kms^{-1})^2$ K], where the mean molecular weight is taken as 0.59 for

a totally ionized gas. In this temperature range, any local disturbances in the hot gas may be thermally unstable, because the radiative cooling rate increases with decreasing T. We therefore assume that the instability promotes the development of a two-phase structure in the gas (Fall & Rees 1985), so that it is the cool gas clouds, being pressure-confined by the surrounding hot gas, that produce Lyα absorptions, as proposed by Mo (1994). In this work, we will be concerned with Lyα lines with low HI column density as $N_{\rm HI} \lesssim 10^{16}$ cm^{-2}, in which the shielding against the UV background radiation is ineffective. The internal density of clouds in the outer parts of halos that give rise to such lines is low enough to be photoionized by the UV background radiation. We thus assume the gas in clouds to be in photoionization equilibrium, where the gaseous temperature is expected to be order of few $\times 10^4$ K, and therefore consistent with the observed Doppler parameters of Lyα lines (see, e.g., Maloney 1992; Rauch et al. 1996).

Note that, even the gas in disks, if disks are formed, will be ionized by the UV radiation in the outer parts, beyond the observed sharp edge at $N_{\rm HI} \sim$ few $\times 10^{19}$ cm^{-2} (Maloney 1992). The galaxies at low redshift imaged by Barcons et al. (1995) are inferred to give rise to absorption lines at an impact parameters of $\gtrsim 50h^{-1}$ kpc, where $H_0 = 100h$ km s^{-1} Mpc^{-1}. The gas which is responsible for such absorption lines is certainly ionized by the UV background radiation (see also, Morris et al. 1993; Salpeter and Hoffmann 1995).

2.2. *H I column density*

We assume that the density profile of both mini and galactic halos is represented by that of a softened isothermal sphere,

$$\rho = \frac{\tilde{\rho} r_c^2}{r^2 + r_c^2} \,, \tag{1}$$

where $\tilde{\rho}$ is the central density and r_c is the core radius. The baryonic gas amounts to a fraction F of the total mass of the halo. Then, the circular velocity $V_c(r)$ at r can be written as,

$$V_c^2(r) = \frac{GM(r)}{r} = 4\pi G \tilde{\rho} r_c^2 \frac{1}{x}(x - \arctan x) \,, \tag{2}$$

where $x \equiv r/r_c$. This functional form of $V_c(r)$ assures a nearly flat rotation curve at large radii $r \gg r_c$. In what follows, the circular velocity is characterised by its value at the virial radius of the halo, r_{vir} (see below for an explanation of r_{vir}). Then, substituting eq.(2) into eq.(1) and introducing $x_v \equiv r_{vir}/r_c$, the density profile of a halo that includes both baryonic gas and dark matter is re-written as,

$$\rho(r, V_c) = \frac{V_c^2}{4\pi G(r^2 + r_c^2)} \Big(\frac{x_v}{x_v - \arctan x_v} \Big) \,, \tag{3}$$

where V_c is the circular velocity at $r = r_{vir}$.

We model the gas in minihalos ($V_1 \leq V_c \leq V_2$) to be in photoionized equilibrium with the external UV background radiation. We write the intensity of the UV background radiation at the

Lyman limit as $J = J_{-21}10^{-21}$ erg cm^{-2} s^{-1} sr^{-1} Hz^{-1}. Using the ionization and recombination rates for a fiducial UV spectrum of $J_\nu \propto \nu^{-1}$ (Black 1981), the H I number density n_{HI} in minihalos is written as,

$$n_{HI} = \frac{\alpha_H(T)}{4\pi J_{-21}10^{-21}G_H}\Big(\frac{F\rho}{m_p}\Big)^2 \qquad \text{for minihalos}\,, \tag{4}$$

where $G_H = 2.54 \times 10^8$ for hydrogen and α_H is the recombination rate coefficient (Black 1981). The column density of H I at an impact parameter b is then estimated as

$$\begin{aligned} N_{HI}(b) &= 2\int_b^\infty \frac{n_{HI}r}{\sqrt{r^2-b^2}}dr \\ &\sim 3.2\times 10^{14}\Big(\frac{T}{3\times 10^4 K}\Big)^{-3/4}\Big(\frac{F}{0.05}\Big)^2 J_{-21}^{-1}\Big(\frac{V_c}{30kms^{-1}}\Big)^4 \\ &\times \Big(\frac{x_v}{x_v - \arctan x_v}\Big)^2 \frac{1}{[(b/10kpc)^2+(r_c/10kpc)^2]^2} \quad \text{cm}^{-2} \quad \text{for minihalos}\,. \end{aligned} \tag{5}$$

For galactic halos ($V_2 \le V_c \le V_3$), we assume a cloud confined by ambient hot gas to be a uniform sphere with proton number density n_{cl} and temperature T_{cl}. The pressure balance with hot gas with proton number density n ($= F\rho/m_p$) and temperature T yields $n_{cl} = nT/T_{cl}$. Under the assumption that the clouds are photoionized by the external UV background and in ionization equilibrium, the H I number density n_{HI} is then written as

$$n_{HI} = \frac{\alpha_H(T_{cl})n_{cl}^2}{4\pi J_{-21}10^{-21}G_H} \propto J_{-21}^{-1}\alpha_H(T_{cl})\Big(\frac{T}{T_{cl}}\Big)^2 n^2 \qquad \text{for galactic halos}\,. \tag{6}$$

The cloud radius R_{cl} for the mass of each cloud M_{cl} is

$$R_{cl} = \Big(\frac{3M_{cl}}{4\pi n_{cl}m_p}\Big)^{1/3} \propto M_{cl}^{1/3}\Big(\frac{T}{T_{cl}}\Big)^{-1/3} n^{-1/3}\,. \tag{7}$$

Each cloud produces the H I column density as $N_{HI}(r) \sim n_{HI}(r)R_{cl}(r)$. In order to obtain the H I column density observed at an impact parameter b from the galactic center, it is required to know the spatial distribution of clouds in halos *a priori*. Without going into details for modeling this, we assume that the clouds have roughly unit covering factor in halos when projected onto the sky, and that each sightline encounters only one cloud in average, which is not in disagreement with the observational results (Morris et al. 1993; LBTW). Then, as we argue in the Appendix, the average H I column density observed at an impact parameter b is well approximated by $N_{HI}(r \to b)$. We thus obtain from eq.(6) and (7)

$$\begin{aligned} N_{HI}(b) &\sim 9.6\times 10^{15}\Big(\frac{M_{cl}}{10^6 M_\odot}\Big)^{1/3}\Big(\frac{T_{cl}}{3\times 10^4 K}\Big)^{-29/12}\Big(\frac{F}{0.05}\Big)^{5/3} J_{-21}^{-1}\Big(\frac{V_c}{200kms^{-1}}\Big)^{20/3} \\ &\times \Big(\frac{x_v}{x_v - \arctan x_v}\Big)^{5/3} \frac{1}{[(b/100kpc)^2+(r_c/100kpc)^2]^{5/3}} \quad \text{cm}^{-2} \quad \text{for galactic halos}\,, \end{aligned} \tag{8}$$

where we assume the virial temperature for T of the hot gas. We note that both expressions for N_{HI} given in eq.(5) and (8) are approximately connected continuously at the canonical value

of $V_c \sim 55$ km s^{-1} for V_2, corresponding to the virial temperature of $T \sim 10^5$ K; this is the temperature of hot gas below which the picture of a two-phase structure in the gas becomes invalid. We therefore use eq.(5) for $V_c < 55$ km s^{-1} and eq.(8) for $V_c \geq 55$ km s^{-1} in the following.

According to several determinations of the intensity of the UV background radiation (e.g. Madau 1992), J_{-21} is nearly constant at high redshifts $2.5 \lesssim z \lesssim 3.5$, whereas at low redshifts $z \lesssim 2.5$ it rapidly decreases with decreasing redshift. We adopt the following functional form for J_{-21},

$$J_{-21}(z) = \begin{cases} \tilde{J}_{-21} & \text{for } z \geq 2.5 \\ \tilde{J}_{-21}\left(\frac{1+z}{3.5}\right)^{\alpha} & \text{for } z < 2.5\,, \end{cases} \tag{9}$$

where the index α quantifies the decreasing rate of J_{-21} for $z < 2.5$.

To estimate the value of $x_v(= r_{vir}/r_c)$ in eq.(3), we use the theory of the spherical collapse of cosmological density perturbations, that yields $r_{vir} = 0.1H_0^{-1}(1+z)^{-3/2}V_c$ for the Einstein-de Sitter (EdS) universe (e.g. Peebles 1980; Padmanabhan 1993). This allows us to derive x_v using the observed values of V_c and r_c of the present-day dark matter halos at $z = 0$. For this purpose, it is convenient to use dark-matter dominated dwarf spirals (Moore 1994), where the dynamical effect of a luminous component on the observed rotation curve is sufficiently small, so that one can accurately determine the structural parameters of dark halos. Adopting the values of V_c and r_c from Moore (1994) for dwarf spirals of DDO154, DDO170, DDO105 and NGC3109, we obtain $10 \lesssim x_v \lesssim 20$ for the EdS universe with $h = 0.5$. In what follows, we assume $x_v = 15 = const.$, since the following results in the concerned low-column density range of $N_{HI} \lesssim 10^{16}$ cm^{-2} are quite insensitive to the values of x_v as long as $x_v \gg 1$.

Figure 1(a) shows the impact parameter b *vs.* the total mass of halos M at $z = 0.5$, where we take $T = 3 \times 10^4$ K for the gas in minihalos (eq.5), $T_{cl} = 3 \times 10^4$ K and $M_{cl} = 10^6 M_{\odot}$ for the clouds in galactic halos (eq.8), with the common parameters of $F = 0.05$, $\tilde{J}_{-21} = 1$, $\alpha = 2$, and $x_v = 15$. It is seen that lines of constant N_{HI} have the slightly different slope at $M \lesssim 2.3 \times 10^{10} M_{\odot}$ (or $V_c \lesssim 55$ km s^{-1}) from that at larger M or V_c. This is because $N_{HI} \propto b^{-3}$ in eq.(5) while $\propto b^{-10/3}$ in eq.(8) for $b \gg r_c$. Here we note that the discontinuities at the boundary of both regimes (at $V_c \sim 55$ km s^{-1}) are quite small in b so that these will not affect the later results. We also find that H I column densities as low as $N_{HI} \sim 10^{14}$ cm^{-2} can be provided by either the low-mass minihalos with the impact parameter b below ~ 40 kpc or by the high-mass galactic halos with larger b. This is more clearly presented in Fig.1(b) that shows N_{HI} *vs.* b for a given total mass M. Dotted line denote the observed size of gaseous envelopes $\sim 160\ h^{-1}$ kpc in luminous galaxies which give rise to Lyα absorptions at $z \lesssim 1$ (LBTW). In our model of absorbers, this is achieved for a mass range of $10^{11} \lesssim M \lesssim 10^{12}\ M_{\odot}$, which corresponds to galaxies with luminosity $10^9 \lesssim L \lesssim 10^{10}\ L_{\odot}$ for the baryon fraction F of 0.05 and the mass-to-light ratio of the order of 5. Thus, the model yields the right order of the size of extended Lyα-absorbing gaseous envelopes in galaxies.

Bold solid line in Fig.1(b) corresponds to the observed correlation between the H I column density and impact parameter by LBTW, assuming Doppler parameters of absorption lines in the

range of $20-40$ km s^{-1}. The present model also implies the correlation and agrees approximately with LBTW, where the slight discrepancy in the slope may be due to the effects of sampling over different galactic masses and/or impact parameters. Recently Le Brun et al. (1996) and Bowen et al. (1996) claimed that the equivalent width of Lyα lines do not correlate with the impact parameter. This has been argued to weaken the possibility of Lyα lines being directly associated with galaxies. The other possibilities discussed in the literature include the scenario of filaments between luminous galaxies, and Lyα lines from outflows from galaxies. The issuse may be settled by assembling the statistically meaningful number of Lyα absorber-galaxy pairs and by comparing with the current type model that presents the explicit dependence of an impact parameter on the masses of galaxies and redshifts (Fig.1c).

2.3. *Cosmological context*

With the knowledge of the H I column density that is produced at an impact parameter $b(N_{\rm HI}, V_c)$, we can calculate the number of Lyα lines with a column density larger than $N_{\rm HI}$, if the number density of halos with circular velocity V_c is known. We use the Press-Schechter formalism for this purpose, and CDM models of structure formation (similar to the work of Mo et al. 1993).

For the EdS universe, the circular velocity V_c and mass M of a CDM halo are related as

$$M = \frac{4\pi}{3}\,\rho_0 r_0^3\,, \qquad V_c = 1.67\,(1+z)^{0.5}\,H_0 r_0\,, \tag{10}$$

where ρ_0 is the present-day mean density of the universe and r_0 is the comoving radius of the halo. The comoving number density of halos per unit circular velocity V_c is given by (Mo et al. 1993)

$$\begin{aligned} n(V_c, z)\,dV_c &= \frac{-3(1.67)^3\,\delta_c\,H_0\,(1+z)^{5/2}}{(2\pi)^{3/2}\,V_c^4\,\Delta(r_0)}\,\frac{d\ln\Delta}{d\ln V_c} \\ &\times\ \exp\Big(\frac{-\delta_c^2(1+z)^2}{2\,\Delta^2(r_0)}\Big)\,dV_c\,. \end{aligned} \tag{11}$$

Here $\Delta(r_0)$ and $\delta_c = 1.68$ are the rms and threshold linear overdensities in a spherical region of radius r_0, respectively, extrapolated to the present epoch. With a top-hat filtering, the functional form of $\Delta(r_0)$ for the CDM power spectrum of density perturbations is taken from Bardeen et al. (1986), and its value is normalized at a scale of $8h^{-1}$ Mpc with the bias parameter b_g.

The number of absorption systems per unit redshift with an H I column density larger than $N_{\rm HI}$, that is produced in halos with circular velocity $V_l < V_c < V_u$, is then given as (Sargent et al. 1980; Mo et al. 1993),

$$\frac{dN(N_{\rm HI}, z, V_l, V_u)}{dz} = \frac{c}{H_0}(1+z)^{1/2}\int_{V_l}^{V_u} dV_c \epsilon n(V_c, z)\pi b^2(N_{\rm HI}, V_c)\,, \tag{12}$$

for the EdS universe. We define $(V_l, V_u) = (V_1, V_2)$ for minihalos and (V_2, V_3) for galactic halos. Here ϵ denotes the fraction of halos that give rise to Lyα absorptions, in view of the fact that

some fraction of halos, specifically early-type galaxies such as E, S0, dE and dS0 in the scale of galactic halos, are lacking of interstellar gas. Since these galaxies experienced the burst of star formation and the subsequent gas loss via galactic wind for only a short period of $\lesssim 1$ Gyr (see e.g. Yoshii & Arimoto 1987), the probability of a sightline to pass the protogalactic, gas-rich stage of these galaxies may be small. To evaluate ϵ, we adopt the nominal fraction 69% of late-type galaxies among all types derived by Postman and Geller (1984) and assume it to be constant with z for simplicity. Thus,

$$\epsilon = \begin{cases} 1 & \text{for mini halos} \\ 0.69 & \text{for galactic halos} . \end{cases} \tag{13}$$

Then the above equation can be used to find the fraction of Lyα lines with $\geq N_{\rm HI}$ that are associated with galactic halos:

$$f_g \equiv \frac{\text{galactic}}{\text{mini} + \text{galactic}} = \frac{dN(N_{\rm HI}, z, V_2, V_3)/dz}{dN(N_{\rm HI}, z, V_1, V_3)/dz} . \tag{14}$$

Besides the case of the 'standard' EdS universe, we will also calculate the number of Lyα lines dN/dz and their galactic fraction f_g for a world model with a cosmological constant. The basic cosmological parameters that define the evolution of the universe are the density parameter $\Omega_0 \equiv \rho_0/\rho_c$, where ρ_c is the critical density to close the universe, and the cosmological constant $\lambda_0 \equiv \Lambda c^2/3H_0^2$. We investigate a low-density ($\Omega_0 < 1$), flat ($\Omega_0 + \lambda_0 = 1$) universe, since such a universe deserves special attention to solve several paradoxical results of cosmological observations (Ostriker & Steinhardt 1995). We use the corresponding set of equations (10)-(12) derived from the spherical collapse theory of density perturbations in a non-zero λ_0 universe (see Peebles 1980 and Suto 1993 for details). The model universes which we adopt for the following analysis are $(\Omega_0,\ \lambda_0,\ h) = (1,\ 0,\ 0.5)$ and $(0.4,\ 0.6,\ 0.65)$. Both universes yield the cosmological age as $\simeq 13$ Gyr, so that any differences in the final results, which may arise from the different cosmological age, are eliminated.

3. MODEL RESULTS

3.1. *The number of absorption lines*

We first calculate the number of Lyα absorption lines based on the model described in the last section, and investigate whether or not the model results can be reconciled with observations.

Figure 2(a) shows the redshift evolution of the number of Lyα absorption lines with an H I column density larger than $N_{HI} = 10^{14}$ cm^{-2}. The absorption lines arise from both minihalos and galactic halos, and the bounds on circular velocities are taken as $V_1 = 15$ km s^{-1} and $V_3 = 250$ km s^{-1}. We take a standard set of parameters for photoionized gas ($T = 3 \times 10^4$ K for minihalos, $T_{cl} = 3 \times 10^4$ K and $M_{cl} = 10^6 M_\odot$ for galactic halos, with $F = 0.05$ and $\tilde{J}_{-21} = 1$). Solid lines correspond to a 'standard' EdS universe ($\Omega_0 = 1,\ \lambda_0 = 0$), while dotted lines to a low-density

($\Omega_0 = 0.4$), flat ($\Omega_0 + \lambda_0 = 1$) universe. It is found, as was already argued by Mo et al. (1993), that there are two stages in the evolution of the number density. First, the rapid formation of minihalos inherent in the CDM models gives rise to the abundant of Lyα lines at $z \gtrsim 10 - 20$, and second, at lower redshifts of $z \lesssim 10$, the number of Lyα lines decreases with time as the hierarchical mergings proceed — small-sized, less-massive objects disappear by being incorporated into larger, more massive objects. The rapid decrease of dN/dz with decreasing z is now an observationally established fact, first recognized by Peterson (1978). For the cases of large b_g and non-zero λ_0, the maximum value of dN/dz is reduced and the epoch at which it is realized is delayed. This is because the growth of density perturbations and subsequent mergings are suppressed due to the bias in galaxy formation and the rapid expansion of the universe. However, the effects of these different assumptions on model parameters appear to be almost indistinguishable at the second stage of the number evolution of Lyα lines. This indicates that probing world models by dN/dz of absorption systems in the observed redshift region of $z \lesssim 3$ may not be useful in view of some model uncertainties. We note here that numerical simulations with a variety of world models have shown almost similar H I column density distribution for Lyα lines (Miralda-Escudè et al. 1995; Hernquist et al. 1995). Also plotted in the figure as filled squares are the observed numbers of Lyα lines at $z \sim 3$ (Petijean et al. 1993), $z \sim 1.5$ (Lu et al. 1991), and $z \sim 0$ (Bahcall et al. 1993). It is clear that the models with $J_{-21} \sim 1 = const.$ at $z \gtrsim 2.5$ are reasonably in agreement with the observed values in the corresponding range of redshifts, whereas the *Hubble Space Telescope* (HST) result of the unexpectedly large number of low-redshift Lyα lines (Bahcall et al. 1993), compared to the extrapolated value from high z, can be explained if the UV flux is decreasing with time (Mo et al. 1993). We find that $J_{-21} = [(1+z)/3.5]^{\alpha}$ with $\alpha \sim 2$ fits well. It is interesting to note that with such a redshift evolution, the current UV flux is $J_{-21}(z=0) \sim 8 \times 10^{-2}$, which is consistent with the observations of Maloney (1992) and Kulkarni and Fall (1993).

The dependence of dN/dz on the column density N_{HI} is shown in Fig.2(b), where filled squares are taken from Rauch et al. (1992) for $2 \lesssim z \lesssim 3$. The observed power-law decline of the Lyα lines, $\propto N_{HI}^{-5/3}$, is well reproduced by the model on the basis of the isothermal density profile of minihalos (Rees 1986), together with the current model of pressure-confined clouds in galactic halos. We remark that this is the case as long as the effect of self-shielding against the external UV radiation is neglected. The effect, leaving a cooled neutral core in the inner part of a sphere (e.g. Chiba & Nath 1994), is realized at the high column-density ends of $N_{HI} \gtrsim 10^{17-18}$ cm^{-2}. This effect is thus unimportant in the present study of low column-density Lyα lines of $10^{14} \lesssim N_{HI} \lesssim 10^{16}$ cm^{-2} that occur at the large impact parameters of sightlines (Fig.1).

3.2. *Fraction of Lyα lines associated with galactic halos*

We now investigate what fraction of Lyα lines can be associated with galactic halos where production of metals is possible — the fraction f_g which may be compared to that of Lyα lines associated with metal lines, f_m.

Figure 3(a) shows the evolution of the galactic fraction f_g of Lyα lines with $N_{HI} > 10^{14}$ cm^{-2}, where we assume $V_2 = 55$ km s^{-1} as the boundary value of V_c between minihalos and galactic halos. It is found that initially at high redshifts ($z \gtrsim 20$), most of Lyα lines are provided by minihalos that collapsed early for the CDM-type power spectrum of density perturbations. This leads to the small values of f_g less than 0.2. Then, at $10 \lesssim z \lesssim 20$, the fraction of lines in galactic halos is rapidly increasing with time as a result of the formation of massive halos via hierarchical merging. Finally at $z \lesssim 10$, the value of f_g slowly converges to the current fraction of $0.75 \sim 0.80$. The figure also indicates that the differences arising from the different bias parameters b_g and cosmological parameters (Ω_0, λ_0), which are clearly visible at high redshifts, become less significant at lower redshifts where observations of absorption lines are accessible. All of the predicted galactic fractions f_g at $z \sim 2.5$ are in between the reported values of f_m for metal lines, $f_m \sim 0.5 - 0.6$ (Cowie et al. 1995; Tytler et al. 1995; Womble et al. 1996) and $f_m \sim 0.75$ (Songaila and Cowie 1996).

The dependence of f_g on the column density N_{HI} at $z = 2.5$ is shown in Fig.3(b). There is an indication of the increase of f_g with N_{HI}; it would tend to be 1 at N_{HI} around 10^{20-21} cm^{-2} for damped Lyα clouds. There are no observational support yet for the above behaviour of f_g with N_{HI} and will be a test for the two population model. Recently, Songaila and Cowie (1996) claim that $f_m \sim 0.9$ for $N_{HI} > 1.6 \times 10^{15}$ cm^{-2} and $f_m \sim 0.75$ for $N_{HI} > 3.0 \times 10^{14}$ cm^{-2}, whereas the other observations give a much lower value of f_m. More observations are needed to settle this issue (see also discussion).

As we mentioned in §2, the exact value of V_2, which separates the range of circular velocities into those of minihalos and galactic halos, is yet to be settled from theoretical points of view. For example, even for $V_c \lesssim 55$ km s^{-1} where the virial temperature is $T \lesssim 10^5$ K, some fraction of gas in an inner part of minihalos may be able to cool and form stars, because of self-shielding effects against the external UV background radiation. We thus turn the argument and address the question, as to which range of V_2 is allowed in the light of the Keck results. Figure 4 shows the galactic fraction of Lyα lines as a function of V_2, while $V_1 = 15$ km s^{-1} and $V_3 = 250$ km s^{-1}. Here we note that the change of V_2 is applied to the range of integration in eq.(12) and the definition of ϵ in eq.(13), whereas the range of V_c for the expressions of N_{HI} ($V_c < 55$ km s^{-1} for eq.5 and $V_c \geq 55$ km s^{-1} for eq.8) is unchanged on the theoretical grounds. For the observed fraction of $0.5 \sim 0.75$, the possible value of V_2 to reproduce it is 40 to 60 km s^{-1}. This is rather insensitive to the specific assumptions on the bias parameter b_g, cosmological parameters (Ω_0, λ_0), and the limiting circular velocities (V_1, V_3). However, to set a more robust constraint on the range of circular velocities or masses for mini/galactic halos, further observational determinations of the fraction of Lyα lines associated with metal lines are needed.

3.3. *Metallicity of absorption systems*

Several recent observations have also measured the metal abundances of absorption lines at high redshifts (Cowie et al. 1995; Womble et al. 1996). The presence of heavy elements implies that interstellar gas confined in dark halos has been processed by star formation and subsequent chemical evolution. While there are some alternative possibilities for enriching gas — one representative idea is that IGM as a whole has already been processed on a sub-galactic scale *prior to* formation of collapsed galactic halos (Songaila & Cowie 1996), we present here the hypothesis that enrichment occurs *after* halo formation. We postulate that gas within halos has been cooled quickly enough to fragment into stars, and being enriched. In our model, this is applied to the gas in galactic-sized halos with $V_2 \le V_c \le V_3$, where cooling time is well less than dynamical time (Dekel & Silk 1986; Efstathiou 1992). Here, we attempt to estimate the possible metal abundances of gas in these halos.

Suppose that a halo with V_c at the redshift z is enriched with an average metallicity $Z(V_c, z)$. Here the dependences on V_c and z arise from the fact that the halos with different V_c collapse and form at different epochs, say z_f, leading to different epochs of star formation, say z_{SF}, and that the subsequent chemical evolution starting at z_{SF} yields the metals at the redshift z. Thus an ensemble of these halos with the metallicity $Z(V_c, z)$ contribute to the metal abundance of Lyα lines. Then since the probability for a sightline to encounter galactic halos in the velocity range of $V_2 \le V_c \le V_3$ is given by eq.(12), we arrive at the average metallicity of Lyα lines with H I column density larger than N_{HI}:

$$< Z > (> N_{HI}, z) = \frac{\int_{V_2}^{V_3} dV_c \cdot Z(V_c, z) n(V_c, z) \pi b^2(N_{\rm HI}, V_c)}{\int_{V_2}^{V_3} dV_c \cdot n(V_c, z) \pi b^2(N_{\rm HI}, V_c)} \,. \qquad (15)$$

The actual expression for $Z(V_c, z)$ in each halo is admittedly not straightforward to derive and very model-dependent. Physics involved in it are, e.g. merging history of a population of dark halos, gasdynamical and thermal processes of gas confined in these halos, and history of star formation. While the extensive and sophisticated approaches of incorporating these processes exist (Lacey & Cole 1993; Kauffmann et al. 1993), we adopt a more simplified approach which we believe includes the essential properties of the system to deduce the characteristic values of metal abundance. First, we assume that the formation redshift z_f of the halo with mass M is represented by the collapse epoch of a rms, 1 σ linear density contrast, i.e., if $D(z)$ denotes the growth rate of density perturbation, z_f is derived from $D(0)/D(z_f) = \Delta(M)/\delta_c$, where M is related to V_c from eq.(10). According to Lacey & Cole (1993) on the basis of their extensive analysis of merging halos, this scaling relation appears to hold for the typical formation epoch of the *main parent* halo which had half or more of the present mass M (see their Fig.9 and Fig.10). Realistically the halo formation epoch for a given M is distributed with some probability arising from different amplitudes of density perturbations, but it can be characterised by the collapse epoch of a typical, 1 σ perturbation. Second, gas in a virialized, galactic-sized halo must cool quickly (within a dynamical time) to ensure star formation, so that z_{SF}, the epoch

of star formation, is assumed to be equal to z_f. This is reasonable, because the cooling time in the galactic scales is less than 10^8 yr, which is a negligible time span — much less than the Hubble time — in the cosmological context. Third, concerning the subsequent chemical evolution, we adopt the observed age-metallicity relation of metal-poor halo stars in our Galaxy (Schuster & Nissen 1989), on the grounds that typical sightlines to produce the Lyα lines with low H I column density penetrate the halo gas, from which old halo stars may have formed. The average enrichment rate $\Delta Z/\Delta t$ derived by Schuster & Nissen (1989) is of the order of 10^{-3} Gyr^{-1} for their sample of halo stars. This value is also close to the value from the chemical-evolution model of the halo by Pagel (1989). Therefore, denoting the age of the universe at the redshift z is $t_{age}(z)$, the metallicity Z at z is derived as,

$$Z(V_c, z) = \int_{t_{age}(z_{SF}(V_c,z))}^{t_{age}(z)} \frac{\Delta Z}{\Delta t} dt \; , \tag{16}$$

where following the above arguments, the epoch of star formation, $t_{SF} \equiv t_{age}(z_{SF}(V_c, z))$, depends on V_c and z.

We assume here that at the outer parts of the halo, which concerns us here for the Lyα forest lines, the gradient of metallcitiy is negligible. This is a reasonable assumption because there are indications that star formation in the outer halo of our Galaxy has been slow and, therefore, the chemical evolution (Matteucci and François 1992). If the variation in star formation rate is caused by the variation in the gas collapse time, then this variation is expected to be small in the outer regions of the halo. This assumption is consistent with the observation that the average metallicity is almost constant for Lyα lines with $N_{HI} \lesssim 10^{16}$ cm^{-2} (Cowie et al. 1995, Songaila and Cowie 1996).

Figure 5(a) shows the evolution of the mean abundance for absorption lines with $N_{HI} > 10^{14}$ cm^{-2} (solid and dotted lines). It is found that for $3 \lesssim z \lesssim 5$, the metal abundance significantly increases by more than two orders of magnitude. At $z \sim 2.5$, it is approximately in agreement with the Keck results of [C/H]$= -2.5 \sim -2$. We remark that the adopted age-metallicity relation of a constant enrichment rate overestimates the halo abundance at $z \lesssim 1$: the relation should be applied to stars with metallicity less than 10^{-1} of solar, which is the criterion to separate halos stars from disk stars (Schuster & Nissen 1989). The subsequent formation of halo stars is stopped, and most of the enriched halo gas would fall into the disk — the hypothesis supported for solving the so-called G-dwarf problem in the solar neighborhood (e.g. Yoshii et al. 1996). Thus we assume $\log < Z > /Z_\odot = -1$ as an upper limit for abundance of absorption lines in Fig.5(a), but this does not change our result in the light of the Keck results at $z = 2 \sim 3$. We have also investigated the case when the epoch of star formation t_{SF} is constant, being independent of the mass scale of halos — as was done by Timmes et al. (1995) for damped Lyα systems. We find that the evolution of $< Z >$ based on our prescription of star formation beginning at the collapse epoch of 1 σ density contrasts is essentially the same as the case when $t_{SF} = 1.5 \sim 2$ Gyr.

Also shown in Fig.5(a) with filled circles are the recent findings of Lu, Sargent & Barlow (1996) for the abundances ([Fe/H]) of damped Lyα systems observed with the Keck. Intriguingly,

the median values of abundances in such systems are well reproduced by the current models. This may support the hypothesis, first proposed by Lanzetta, Wolfe & Turnshek (1995a), that damped Lyα systems could represent a spheroidal component of galaxies (see discussion in §4.2).

The dependence of $< Z >$ on the value of V_2 is shown in Fig.5(b). In contrast with the galactic fraction f_g of Lyα lines, $< Z >$ turns out to be sensitive to both the bias parameter b_g and the cosmological parameters (Ω_0, λ_0) at large values of V_2. It is systematically lower for a larger bias and/or lower-density universe. This is caused by delayed star-formation epoch t_{SF}, leading to less time for enriching gas.

4. DISCUSSION AND CONCLUDING REMARKS

4.1. *Evolution of galactic fraction and average metallicity*

We have shown that the observed fraction of Lyα absorption lines associated with metal lines can be understood in terms of photoionized gas confined in galactic-sized halos with $40-60 \lesssim V_c \lesssim 250$ km s^{-1}, whose number density follows the Press-Schechter model of hierarchical structure formation. The derived average abundance of heavy elements in absorption systems, combined with the characteristic epochs of star formation and the observed age-metallicity relation in our Galactic halo, appears to be reasonably in agreement with the observed abundance at $z = 2 \sim 3$.

The current model also suggests that both the fraction of Lyα lines associated with galactic halos and the metallicity in absorption systems are expected to increase with decreasing redshift (Fig.3a and Fig.5a). While the explicit dependences of these quantities on redshift are yet to be settled (see Songaila & Cowie 1996), we note the findings of Steidel (1990) that the number density of C IV lines increases with decreasing redshift. In our model, this can be explained from the above predicted properties of absorption systems in the following way.

In photoionization equilibrium, the ratio between the column densities of C IV and H I is a function of the ionization parameter Γ, which is the ratio of the densities of ionizing photons and particles, and of the metallicity Z; using the photoionization code of CLOUDY (Ferland 1993), we find that for $\log_{10}\Gamma = -1.5$ to -2.0, and for $Z = 0.001$ to 0.5, the ratio N_{CIV}/N_{HI} is well described as,

$$\frac{N_{CIV}}{N_{HI}} \propto \Gamma^{-1.3\pm0.2} Z^{1.0\pm0.1} . \tag{17}$$

Then, suppose that the number density of Lyα lines per unit H I column density and redshift, $d^2\bar{N}_{HI}/dN_{HI}dz$, is represented by a power law form,

$$\frac{d^2\bar{N}_{HI}}{dN_{HI}dz} dN_{HI}dz \propto N_{HI}^{-\beta}(1+z)^{\gamma} dN_{HI}dz , \tag{18}$$

where $\beta \sim 1.5$ (Sargent et al. 1989) and $\gamma \sim 2.45$ (Lu et al. 1991), and that a fraction f_g of these

Lyα lines are associated with C IV lines, which may be written as,

$$f_g(z) \propto (1+z)^{-\eta} \,. \tag{19}$$

From Fig. 3(a), we obtain $\eta \sim 1.6$ at $z = 2 \sim 3$.

Suppose also that the mean metallicity of absorption lines increases in time following $< Z > \propto (1+z)^{-\delta}$. Then eq.(17) and eq.(18) give the column density distribution of C IV lines as,

$$\frac{d^2 \bar{N}_{CIV}}{dN_{CIV} dz} dN_{CIV} dz \propto N_{CIV}^{-\beta} (1+z)^{\gamma_C} dN_{CIV} dz \,, \tag{20}$$

where

$$\gamma_C = \gamma - \delta(\beta) - \eta \,, \tag{21}$$

describes the redshift evolution of C IV lines. It is known from observations that the β index is the same for both H I and C IV lines (Cowie et al. 1995; Bergeron et al. 1994), indicating that the simple equation (17) holds well.

Steidel (1990) has shown that the index γ_C is negative, of order -1.25. This means that the number of C IV lines increases in time. In our model, this can be due partly to the increase of the galactic fraction f_g in time and to the increase of the metallicity $< Z >$ in time. Then, for the set of power-law indices, $\beta = 1.5$, $\gamma_C = -1.25$, $\gamma = 2.45$, and $\eta = 1.6$, we arrive at $\delta = 1.4$, thereby indicating,

$$< Z > \propto (1+z)^{-1.4} \,. \tag{22}$$

It is worth noting that the enrichment rate of absorption lines shown in Fig.5(a) is well approximated by this equation. The redshift evolution for C IV lines used here is, strictly speaking, for high C IV column density lines. It will be interesting to see whether observations in the near future show a similar redshift evolution for small C IV column density lines.

Therefore, the derived redshift evolutions of both the fraction of Lyα lines associated with galactic halos (Fig.3a) and the metallicity in absorption systems (Fig.5a) are approximately consistent with the observed scaling laws for Lyα and C IV lines.

4.2. *Possible relation with metals in damped Lyα systems*

The abundances of metals have also been measured in damped Lyα systems, which are believed to be protogalaxies. Smith et al. (1996) and Pettini et al. (1995) have recently reported, by measuring the Zn lines as a probe of metallicity, that the typical Zn abundance at $z \sim 2$ is 1/15 of solar, but there is a considerable scatter in the Zn abundance, spanning more than two orders of magnitude. Using high quality spectra obtained with the Keck telescope, Lu, Sargent & Barlow (1996) have also derived a large scatter of abundances, about a factor of 30, with N_{HI}-weighted mean abundance of 0.028 solar between $2 < z < 3$. In the context of the present

model, such a large scatter may be caused by the different formation epoch of halos, z_f, for a given mass arising from the different amplitudes of primordial density fluctuations and different merging history (Lacey & Cole 1993). Also, for the adopted age-metallicity relationship of halo stars, there is a scatter in the ages of the stars of ± 2.5 Gyr at a given abundance, leading to a scatter of abundances more than an order of magnitude at a given age (Schuster & Nissen 1989). It is worth noting that the evolution of the mean abundance is reproduced from the formation epoch of a typical 1 σ fluctuation and the mean age-metallicity relationship of halo stars in our Galaxy (Fig.5a). This suggests that damped Lyα systems represent a metal-poor halo component. Also, Songaila and Cowie (1996) found that the ratio Si/C is about three times solar, similar to the abundance ratio of Galactic halo stars.

4.3. *The possibility of an enriched IGM*

The two population model, as presented here, clearly predicts (a) the fraction of Lyα lines with associated metal lines as a function of redshift and (b) the redshift evolution of the average metallicity. The observations, however, have not yet converged to any firm conclusion and it is too early to rule out other possibilities. As noted in Songaila and Cowie (1996), it will be very difficult to determine the fraction of metal enriched Lyα clouds below $N_{HI} \lesssim 10^{15}$ cm^{-2}, because this will mean a sensitivity limit of $N_{CIV} \lesssim 10^{11}$ cm^{-2}, which is difficult at present. They claim to have found associated C IV lines in 90% of clouds with $N_{HI} > 1.6 \times 10^{15}$ cm^{-2} and 75% of clouds with $N_{HI} > 3.0 \times 10^{14}$ cm^{-2}. If confirmed, such a large fraction of enriched clouds will be difficult to explain with the two population model. As emphasized by Songaila and Cowie (1996), the alternative hypothesis of an enriched IGM will then be more appropriate.

We briefly note here that a problem also prevails at low redshifts about the interpretation of the fraction of Lyα lines with associated metal lines. Although the association of some of the low column density Lyα lines with galaxies seems sure, it is still uncertain as to how physical the association is (see Le Brun et al. 1996 for a discussion). It is possible that instead of being directly associated with galactic halos (as in, for example, Mo and Morris 1994), the Lyα lines trace some structure related to formation of galaxies (Morris and van den Bergh 1994, Petitjean et al. 1995).

We note here the possibility, as shown in several recent numerical simulations (Miralda-Escudè et al. 1995, Hernquist et al. 1995) that very low column density Lyα lines may arise in mini pancakes and not minihalos. In this case, the density profile will be much different and our results may not hold. However, we note that mini pancakes can account for Lyα lines with $N_{HI} \lesssim 10^{15}$ cm^{-2} (Miralda-Escudè et al. 1995) and lines with higher H I column density come from the intersecting points of pancakes, and correspond to minihalos or galactic halos of our model. Therefore, our results are most certain to hold for $N_{HI} \gtrsim 10^{15}$ cm^{-2}. In any case, as explained above, the fraction of Lyα lines with associated metal lines for $N_{HI} \lesssim 10^{15}$ cm^{-2} will be difficult to determine in the near future, and our model will not be testable for such values of H I column densities.

Incidentally, the case for an enriched IGM was described by Silk et al. (1987) much before the discovery of associated metal lines in Lyα systems. They discussed the possibility of enriching the IGM by galactic winds from dwarf galaxies. The detail of such a scenario, however, remains to be worked out. Pregalactic objects such as Population III stars might also enrich the IGM at high redshifts, but again no detail models exist.

In the face of such interesting but still poorly understood scenarios, it therefore seems reasonable to pursue a modified version of the minihalo model, such as the two population model presented here. We have shown that a fraction of $\gtrsim 0.5$ of Lyα forest lines with associated metal lines can be understood in the framework of hierarchical structure formation model, assuming that halos with velocity dispersion $15 \lesssim V_c \lesssim 55$ km/s do not produce stars and heavy elements. The model predicts that the fraction of clouds with associated metal lines increases slowly with the H I column density. We have shown that the results are robust and do not depend strongly on the assumptions of the limiting values of velocity dispersion. We have further used the age-metallicity relation of Galactic halo stars to predict the evolution of the average metallicity of the associated metal line systems. In particular, we find that the average metallicity at $z \sim 2$ should be about a hundredth of solar.

We thank T. Padmanabhan, R. Srianand, and E. J. Wampler for stimulating discussions and helpful comments. We are also grateful to the referee for his constructive suggestions for the improvement of this paper. This work has been supported in part by the Grand-in-Aid for Scientific Research (08640318) of the Ministry of Education, Science, and Culture in Japan.

A. N_{HI} vs. b in galactic halos

We describe below how to obtain the H I column density as a function of the impact parameter b for Lyα-absorbing gas clouds in galactic halos.

The probability Pdl that a sightline in the range of $l \sim l + dl$ encounters the clouds confined in the ambient hot gas is given as $Pdl = n_s \sigma dl$, where n_s is the number density of clouds and $\sigma \equiv \pi R_{cl}^2$ is the cross section of each cloud. Under the assumption that each sightline encounters one cloud in average, P is normalized as $\int Pdl = 1$. Then, if each cloud has its own column density $N_{HI}(r)$ as a function of the galactocentric distance r, the average column density $< N_{HI} > (b)$ at the impact parameter b may be written as,

$$\begin{aligned} < N_{HI} > (b) &= \int_0^\infty N_{HI}(r) n_s \sigma dl \\ &= 2 \int_b^\infty N_{HI}(r) \frac{n_s \sigma r dr}{\sqrt{r^2 - b^2}} \ . \end{aligned} \tag{A1}$$

To obtain the possible expression for n_s, we assume that the whole area of a galactic halo projected onto the sky is in average covered by ensemble of clouds without overlapping. This is

equivalent to $\int Pdl = 1$ as described above. Then, the average number density of clouds within b, denoted as $\bar{n}_s$, may be approximately given as $\bar{n}_s \sim 1/(4\pi R_{cl}^2 b/3)$, and this yields the number density n_s at each b as $n_s \sim 1/(2\pi R_{cl}^2 b)$. Equation (A1) is then reduced to

$$< N_{HI} > (b) = \frac{1}{b}\int_b^\infty N_{HI}(r)\frac{rdr}{\sqrt{r^2-b^2}} \tag{A2}$$

Here we note that $N_{HI}(r) \propto r^{-10/3} \equiv Kr^{-10/3}$ at $r \gg r_c$ where H I column densities of Lyα absorption lines are lower than 10^{16} cm^{-2} in galactic halos. Substituting this into eq.(A2), we obtain

$$< N_{HI} > (b) = \frac{K}{b}\int_b^\infty \frac{r^{-7/3}dr}{\sqrt{r^2-b^2}} = Kb^{-10/3}\int_0^\infty \frac{dx}{\cosh^{7/3}x}\ , \tag{A3}$$

where we introduce the variable x by $r = b\cosh x$ in the second equation. The integration in eq.(A3) yields 0.91, and this can be regarded as ~ 1 in view of the other uncertainties. This allows us to adopt the approximate equality as $< N_{HI} > (b) \sim N_{HI}(r \to b)$.

REFERENCES

Bahcall, J.N., et al. 1993, ApJS, 87, 1

Barcons, X., Lanzetta, K.M., & Webb, J.K. 1995, Nature, 376, 321

Black, J. 1981, MNRAS, 197, 553

Bowen, D.V., Blades, J.C., & Pettini, M. 1996, ApJ, 464, 141

Chiba, M. & Nath, B.B. 1994, ApJ, 436, 618

Cowie, L.L., Songaila, A., Kim, T.S., & Hu, E.M. 1995, AJ, 109, 1522

Cristiani, S., D'Odorico, S., Fontana, A., Giallongo, E., & Savaglio, S. 1995, MNRAS, 273, 1016

Dekel, A. & Silk, J. 1986, ApJ, 303, 39

Efstathiou, G. 1992, MNRAS, 256, 43P

Fall, S.M. & Rees, M.J. 1985, ApJ, 298, 18

Ferland, G.J. 1993, University of Kentucky Department of Physics and Astronomy Internal Report

Fernández-Soto, A., et al. 1996, ApJ, 460, L85

Hernquist, L., Katz, N., Weinberg, D.H. & Miralda-Escudè, J. 1995, submitted to ApJ(astro-ph/9509105)

Ikeuchi, S. 1986, Ap&SS, 118, 509

Kauffmann, G., White, S.D.M., & Guiderdoni, B. 1993, MNRAS, 264, 201

Kulkarni, V., & Fall, S.M. 1993, ApJ, 413, L63

Lacey, C. & Cole, S. 1993, MNRAS, 262, 627

Lanzetta, K.M., Wolfe, A.M., & Turnshek, D.A. 1995a, ApJ, 440, 435

Lanzetta, K.M., Bowen, D.B., Tytler, D., & Webb, J.K. 1995b, ApJ, 442, 538

Le Brun, V., Bergeron, J., Boisse, P. 1996, A&A, 306, 691

Lu, L., Wolfe, A.M., & Turnshek, D.A. 1991, ApJ, 367, 19

Lu, L., Sargent, W.L.W., & Barlow, T.A. 1996, preprint (astro-ph/9606044)

Madau, P. 1992, ApJ, 389, L1

Maloney, P. 1992, ApJ, 398, L89

Matteucci, F., & François, P. 1992, A&A, 262, L1

Miralda-Escudè, J., Cen, R., Ostriker, J.P., & Rauch, M. 1995, submitted to ApJ(astro-ph/9511013)

Mo, H.J., Miralda-Escudè, J., & Rees, M.J. 1993, MNRAS, 264, 705

Mo, H.J., & Morris, S.L. 1994, MNRAS, 269, 52

Mo, H.J. 1994, MNRAS, 269, L49

Morris, S.L., Weymann, R.J., Dressler, A., McCarthy, P.J., Smith, B.A., Terrile, R., Giovanelli, R., & Irwin, M. 1993, ApJ, 419, 524

Morris, S.L., & van den Bergh, S. 1994, ApJ, 427, 696

Moore, B. 1994, Nature, 370, 629

Ostriker, J.P. & Steinhardt, P.J. 1995, Nature, 377, 600

Padmanabhan, T. 1993, Structure Formation in the Universe (Cambridge: Cambridge Univ. Press)

Pagel, B.E.J. 1989, Rev. Mexicana Astron. Astrofis., 18, 161

Peebles, P.J.E. 1980, The Large-Scale Structure of the Universe (Princeton: Princeton Univ. Press)

Peterson, B.A. 1978, in The Large-Scale Structure of the Universe, eds. M.S. Longair, J. Einasto (Dordrecht: Reidel), p. 389

Petitjean, P., Webb, J.K., Rauch, M., Carswell, R.F., & Lanzetta, K. 1993, MNRAS, 262, 499

Petitjean, P., Mücket, J., & Kates, R.E. 1995, A&A, 295, L9

Pettini, M., King, D.L., Smith, L.J., & Hunstead, R.W. 1995, in QSO Absorption Lines, ed. G. Meylan (Berlin: Springer-Verlag), p. 71

Postman, M. & Geller, M.J. 1984, ApJ, 281, 95

Press, W.H., Schechter, P. 1974, ApJ, 187, 425

Rauch, M., Carswell, R.F., Chaffee, F.H., Foltz, C.B., Webb, J.K., Weymann, R.J., Bechtold, J., & Green, R.F. 1992, ApJ, 390, 387

Rauch, M., Sargent, W.L.W., Womble, D.S., & Barlow, T.A. 1996, ApJ, 467, L5

Rees, M.J. 1986, MNRAS, 218, 25P

Salpeter, E. & Hoffmann, G.L. 1995, ApJ, 441, 51

Sargent, W.L.W., Young, P.J., Boksenberg, A., & Tytler, D. 1980, ApJS, 42, 41

Sargent, W.L.W., Steidel, C.C., & Boksenberg, A. 1989, ApJS, 69, 703

Schuster, W.J. & Nissen, P.E. 1989, A&A, 222, 69

Silk, J., Wyse, R.F.G., & Shields, G. A. 1987, ApJ, 322, L59

Smith, L.J., Pettini, M., King, D.L., & Hunstead, R.W. 1996, in The Impact of Stellar Physics on Galaxy Evolution, eds. C. Leitherer, U. F.-v. Alvensleben, J. Huchra, in press

Songaila, A., & Cowie, L.L. 1996, AJ, in press (astro-ph/9605102)

Steidel, C.C. 1990, ApJS, 72, 1

Suto, Y. 1993, Progress of Theoretical Physics, 90, 1173

Thoul, A.A. & Weinberg, D.H. 1996, ApJ, 465, 608

Timmes, F.X., Lauroesch, J.T., & Truran, J.W. 1995, ApJ, 451, 468

Tytler, D., Fan, X.-M., Burles, S., Cottrell, L., Davis, C., Kirkman, D., & Zuo, L. 1995,, in QSO Absorption Lines, ed. G. Meylan (Berlin: Springer-Verlag), p. 289

Womble, D.S, Sargent, W.L.W., & Lyons, R.S. 1996, in Cold gas at High Redshift, eds. M. Bremer, H. Rottgering, P. van der Werf, C. Carilli (Kluwer), in press

Yoshii, Y. & Arimoto, N. 1987, A&A, 188, 13

Yoshii, Y., Tsujimoto, T., & Nomoto, K. 1996, ApJ, 462, 266

Figure Captions

Fig. 1.— **(a)** The impact parameter b (Mpc) of a sightline as a function of the total mass of a halo M ($M_\odot$) to produce an H I column density N_{HI} at $z = 0.5$ ($F = 0.05$, $\tilde{J}_{-21} = 1$, $x_v = 15$, and $h = 1$). The solid lines correspond to $\alpha = 2$ (or $J_{-21} \simeq 0.18$ in eq.9) for $N_{HI} = 10^{14}$, 10^{15}, and 10^{16} cm^{-2} from left to right, respectively. The dashed line corresponds to $\alpha = 0$ (or $J_{-21} = 1$) for $N_{HI} = 10^{16}$ cm^{-2}. These lines are quite insensitive to the adopted cosmological parameters of Ω_0 and λ_0. For comparison, the observed value of $\sim 160\ h^{-1}$ kpc for the size of gaseous halos at $z \lesssim 1$ is plotted as a dotted line (LBTW). **(b)** The H I column density N_{HI} (cm^{-2}) against the impact parameter b (Mpc). The solid lines correspond to $\alpha = 2$ for $M = 10^{10}$, 10^{11}, and 10^{12} $M_\odot$ from left to right, respectively, whereas the dashed line to $\alpha = 0$ for $M = 10^{12}$ $M_\odot$. The other parameters are the same as those in (a). The dotted line is the observed size of gaseous halo $\sim 160\ h^{-1}$ kpc, whereas the bold solid line denotes the reported correlation between N_{HI} and b (LBTW). **(c)** The impact parameter b (kpc) of a sightline as a function of redshift z.

Fig. 2.— **(a)** The redshift evolution of the number of Lyα absorption lines with a column density larger than $N_{HI} = 10^{14}$ cm^{-2} ($F = 0.05$, $\tilde{J}_{-21} = 1$, $x_v = 15$). The range of circular velocities V_c are $15 \leq V_c \leq 250$ km s^{-1} (i.e. $V_1 = 15$ km s^{-1}, $V_3 = 250$ km s^{-1}). Thick and thin lines are for the EdS universe ($\Omega_0 = 1$, $\lambda_0 = 0$, $h = 0.5$) and the non-zero λ_0 universe ($\Omega_0 = 0.4$, $\lambda_0 = 0.6$, $h = 0.65$), respectively, for CDM models with bias parameter $b_g = 1$ (solid lines) and $b_g = 1.3$ (dotted). The different curves at $z \leq 2.5$ corresponds to the different values of α in eq.(6): the upper curves for $\alpha = 2$ and the lower for $\alpha = 0$. Filled squares denote the observed number of Lyα lines at $z \sim 3$ (Petijean et al. 1993), $z \sim 1.5$ (Lu et al. 1991), and $z \sim 0$ (Bahcall et al. 1993). **(b)** The dependence of dN/dz on the H I column density limit for $z = 2.5$ and $b_g = 1$. Filled squares denote the results of Rauch et al. (1992) for $2 \lesssim z \lesssim 3$. The other parameters are the same as those in (a).

Fig. 3.— **(a)** The redshift evolution of the fraction of Lyα absorption lines associated with galactic halos in the range of $55 \leq V_c \leq 250$ km s^{-1} (while $15 \leq V_c \leq 55$ km s^{-1} for minihalos), with $N_{HI} > 10^{14}$ cm^{-2}. The error bar denotes the Keck results for the fraction of Lyα lines associated with CIV metal lines (Cowie et al. 1995; Tytler et al. 1995; Womble et al. 1996; Songaila & Cowie 1996). The meanings of the four curves presented are the same as those in Fig.2(a). **(b)** The dependence of the fraction of Lyα absorption lines associated with galactic halos on the H I column density limit at $z = 2.5$. The others are the same for (a).

Fig. 4.— The dependence of the fraction of Lyα absorption lines associated with galactic halos on the lower bound of the circular velocity V_2 (while $V_1 = 15$ km s^{-1} and $V_3 = 250$ km s^{-1}), for $z = 2.5$ and $N_{HI} > 10^{14}$ cm^{-2}. The meanings of the four curves are the same as those in Fig.2(a). The observed fraction of Lyα lines associated with CIV metal lines, $0.5 \sim 0.75$, is indicated as a bar.

Fig. 5.— **(a)** The redshift evolution of the average metallicity $< Z >$ of absorption lines (solid

curves for $b_g = 1$ and dotted for $b_g = 1.3$), based on the model described in subsection 3.3. The range of circular velocities for galactic halos are $55 \leq V_c \leq 250$ km s^{-1}. For reference, the metallicity evolutions if the star formation commences from the beginning of the universe, $t_{SF} = 0$, are shown as dashed lines. The crossed error bars denote the Keck results for the Lyα lines associated with CIV metal lines ([C/H]) (Cowie et al. 1995; Tytler et al. 1995; Womble et al. 1996), and filled circles denote the abundances of damped Lyα systems ([Fe/H]) observed with the Keck (Lu, Sargent & Barlow 1996). **(b)** The dependence of the average metallicity of absorption lines on the lower bound of the circular velocity V_2 (while $V_3 = 250$ km s^{-1}), at $z = 2.5$.

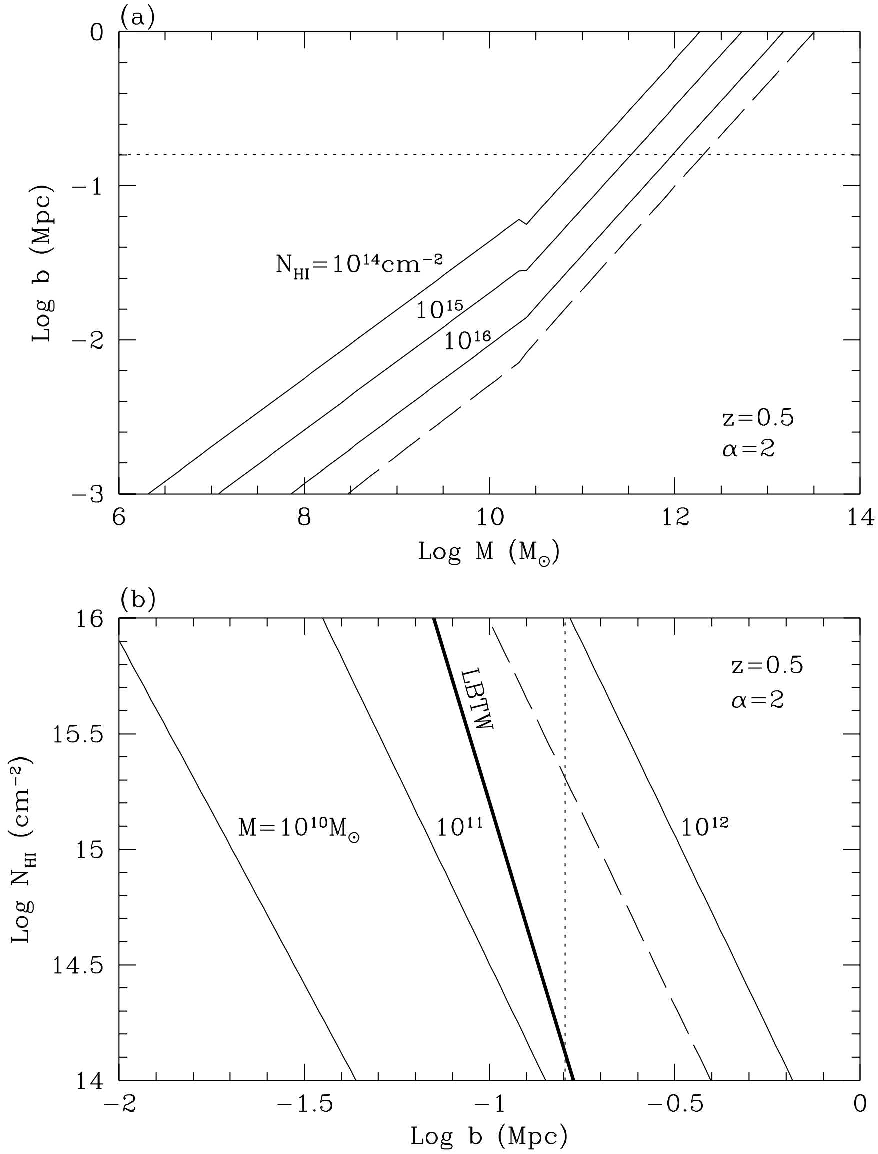
(a)
0
−1
−2
−3
Log b (Mpc)
6
8
10
12
14
Log M (M⊙)
N_HI=10¹⁴cm⁻²
10¹⁵
10¹⁶
z=0.5
α=2
(b)
16
15.5
15
14.5
14
Log N_HI (cm⁻²)
−2
−1.5
−1
−0.5
0
Log b (Mpc)
M=10¹⁰M⊙
10¹¹
LBTW
10¹²
z=0.5
α=2

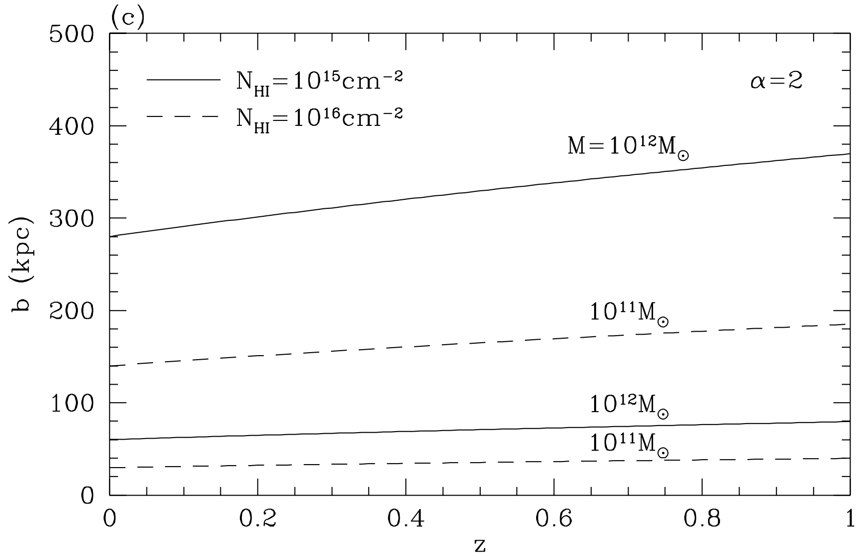
(c)
N_HI=10^15cm^-2
N_HI=10^16cm^-2
α=2
M=10^12M_⊙
10^11M_⊙
10^12M_⊙
10^11M_⊙
b (kpc)
z
0
100
200
300
400
500
0
0.2
0.4
0.6
0.8
1

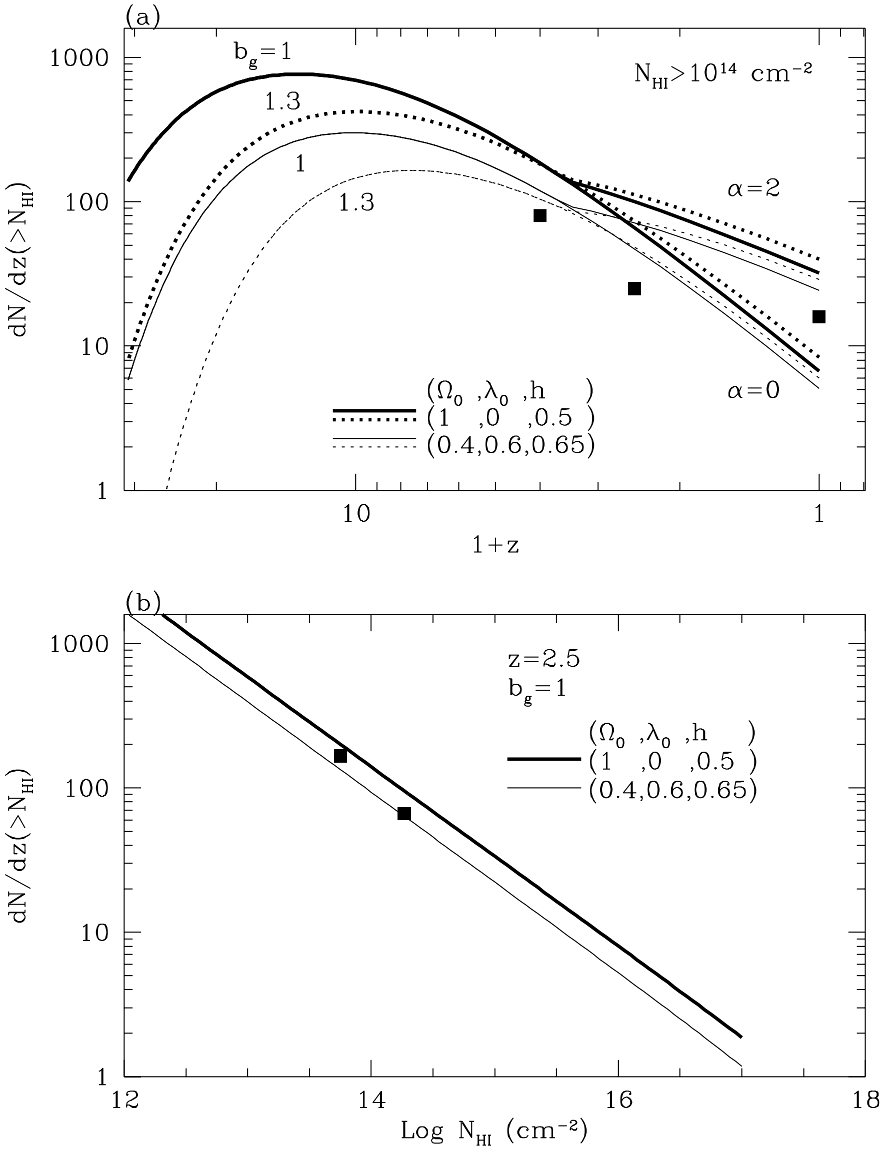
(a)
$b_g=1$
1.3
1
1.3
$N_{HI}>10^{14}$ cm^{-2}
$\alpha=2$
$\alpha=0$
$(\Omega_0\ ,\lambda_0\ ,h\ \ )$
$(1\ \ ,0\ \ ,0.5\ )$
$(0.4,0.6,0.65)$
dN/dz(>N_{HI})
1+z
(b)
z=2.5
$b_g=1$
$(\Omega_0\ ,\lambda_0\ ,h\ \ )$
$(1\ \ ,0\ \ ,0.5\ )$
$(0.4,0.6,0.65)$
dN/dz(>N_{HI})
Log N_{HI} (cm^{-2})

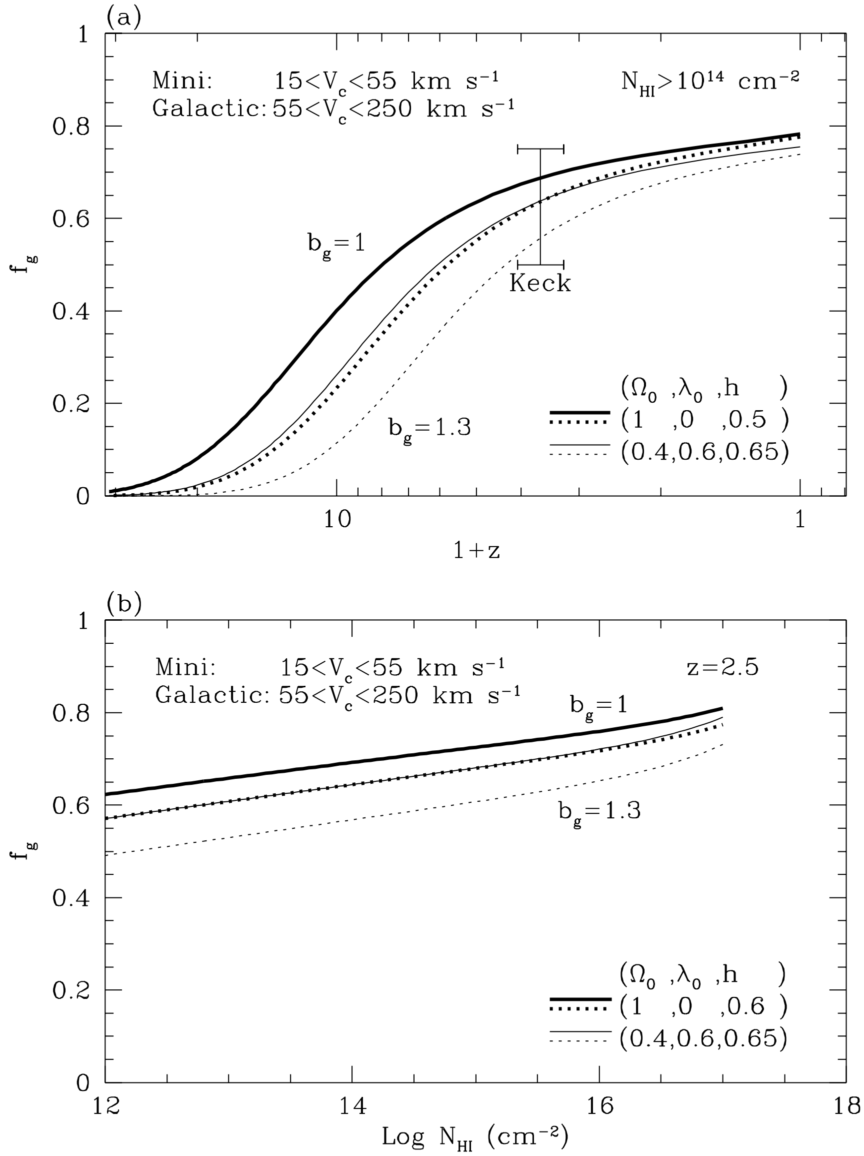
(a)
Mini: 15<V_c<55 km s^-1
Galactic: 55<V_c<250 km s^-1
N_HI>10^14 cm^-2
b_g=1
b_g=1.3
Keck
(Ω_0 ,λ_0 ,h)
(1 ,0 ,0.5)
(0.4,0.6,0.65)
f_g
1+z
(b)
Mini: 15<V_c<55 km s^-1
Galactic: 55<V_c<250 km s^-1
z=2.5
b_g=1
b_g=1.3
(Ω_0 ,λ_0 ,h)
(1 ,0 ,0.6)
(0.4,0.6,0.65)
f_g
Log N_HI (cm^-2)

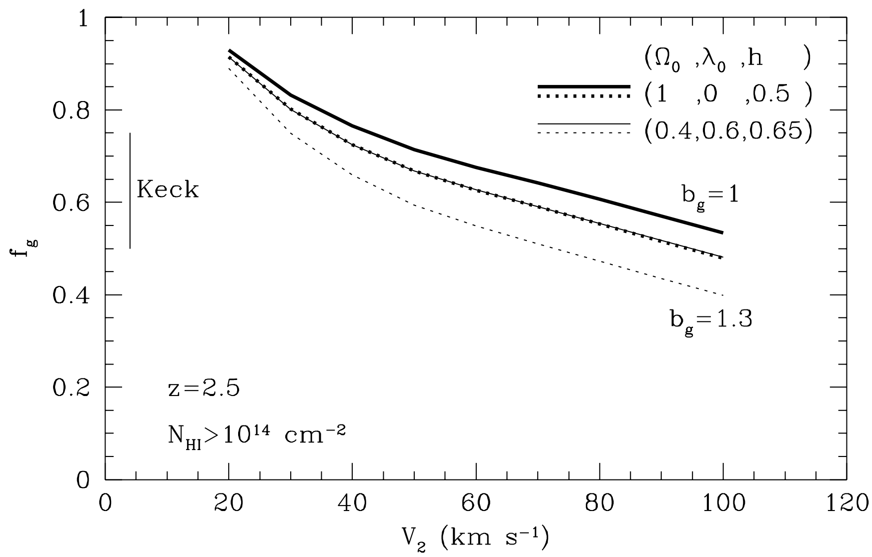

$(\Omega_0\ ,\lambda_0\ ,h\ )$
$(1\ ,0\ ,0.5\ )$
$(0.4,0.6,0.65)$
Keck
$b_g=1$
$b_g=1.3$
$z=2.5$
$N_{HI}>10^{14}\ cm^{-2}$
f_g
V_2 (km s^{-1})
0
0.2
0.4
0.6
0.8
1
20
40
60
80
100
120

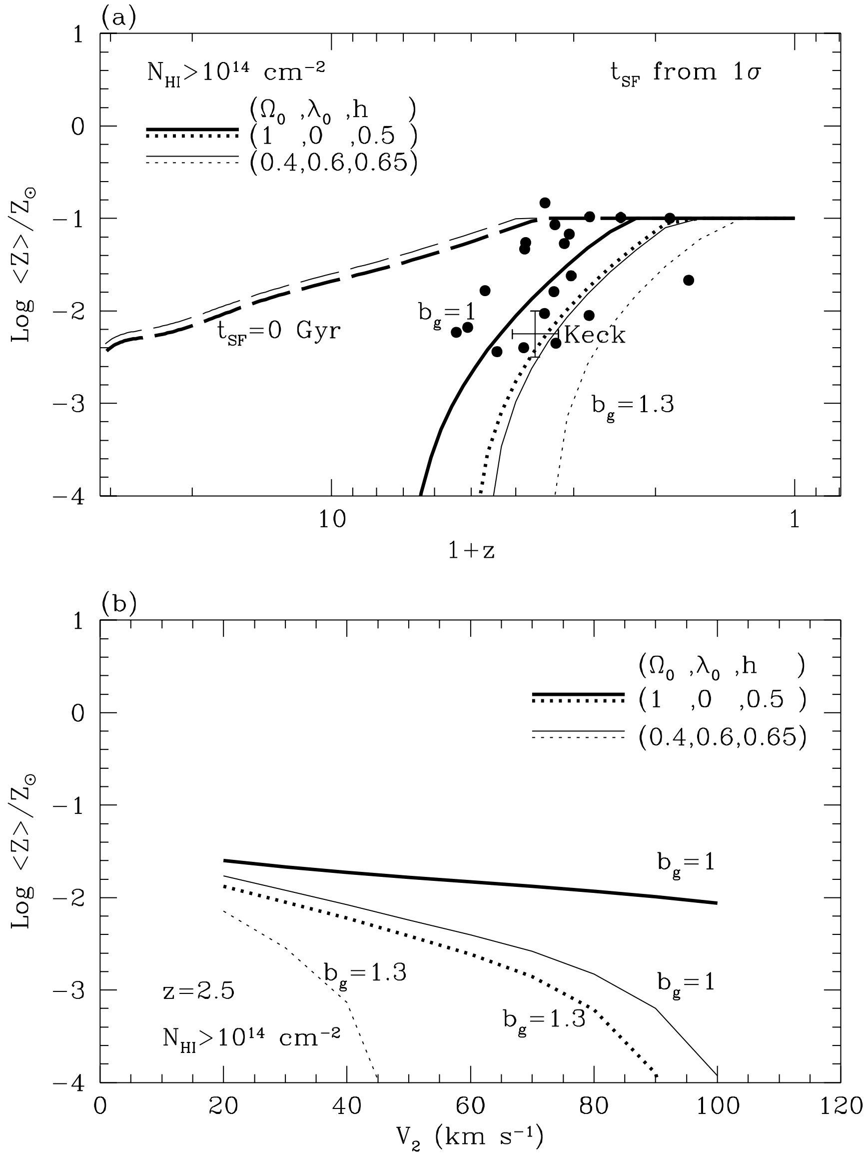
(a)
$N_{HI}>10^{14}$ cm^{-2}
t_{SF} from 1σ
(Ω_0, λ_0, h)
(1 ,0 ,0.5)
(0.4,0.6,0.65)
t_{SF}=0 Gyr
b_g=1
Keck
b_g=1.3
Log <Z>/$Z_\odot$
1+z
(b)
(Ω_0, λ_0, h)
(1 ,0 ,0.5)
(0.4,0.6,0.65)
b_g=1
b_g=1.3
b_g=1
b_g=1.3
z=2.5
$N_{HI}>10^{14}$ cm^{-2}
Log <Z>/$Z_\odot$
V_2 (km s^{-1})